

# Unsupervised Event Detection, Clustering, and Use Case Exposition in Micro-PMU Measurements

Armin Aligholian, *Student Member, IEEE*, Alireza Shahsavar, *Member, IEEE*, Emma Stewart, *Senior Member, IEEE*, Ed Cortez, Hamed Mohsenian-Rad, *Fellow, IEEE*

**Abstract**—Distribution-level phasor measurement units, a.k.a., micro-PMUs, report a large volume of high resolution phasor measurements which constitute a variety of *event signatures* of different phenomena that occur all across power distribution feeders. In order to implement an event-based analysis that has useful applications for the utility operator, one needs to extract these events from a large volume of micro-PMU data. However, due to the *infrequent*, *unscheduled*, and *unknown* nature of the events, it is often a challenge to even figure out what kind of events are out there to capture and scrutinize. In this paper, we seek to address this open problem by developing an *unsupervised* approach, which requires *minimal prior human knowledge*. First, we develop an unsupervised event detection method based on the concept of Generative Adversarial Networks (GAN). It works by training deep neural networks that learn the characteristics of the normal trends in micro-PMU measurements; and accordingly detect an event when there is any abnormality. We also propose a two-step unsupervised clustering method, based on a novel linear mixed integer programming formulation. It helps us categorize events based on their origin in the first step and their similarity in the second step. The active nature of the proposed clustering method makes it capable of identifying new clusters of events on *an ongoing basis*. The proposed unsupervised event detection and clustering methods are applied to real-world micro-PMU data. Results show that they can outperform the prevalent methods in the literature. These methods also facilitate our further analysis to identify important clusters of events that lead to unmasking several use cases that could be of value to the utility operator.

**Keywords:** Micro-PMU, distribution synchrophasors, unsupervised data-driven analysis, event detection, event clustering, deep learning, generative adversarial network, unmasking use cases.

## I. INTRODUCTION

### A. Background and Motivation

Power distribution systems are becoming more active and dynamic due to the increasing penetration of distributed energy sources, electric vehicles, dynamic loads, and etc. This gives rise to various monitoring and control issues. Many of these issues can be addressed by the use of distribution-level phasor measurement units, a.k.a., micro-PMU [1].

One of the emerging applications of micro-PMUs is to study “events” in power distribution systems. Event-based studies of micro-PMU measurements have a wide range of use cases, such as in situational awareness [2], equipment health diagnostics, such as for inverters [3], capacitor banks [4], transformers [5], distribution-level oscillation detection and analysis [6], fault analysis and fault location [7].

A. Aligholian, A. Shahsavar and H. Mohsenian-Rad are with the University of California, Riverside, CA, USA. E. Stewart is with the Lawrence Livermore National Laboratory, Livermore, CA, USA. E. Cortez is with the Riverside Public Utilities, Riverside, CA, USA. This work is supported in part by UCOP grant LFR-18-548175. The corresponding author is H. Mohsenian-Rad.

Before one can do any event-based analysis, including for the above use cases in [2]–[7], one needs to first detect and identify the *events that are of value*. However, this is a challenging task due to at least the following three reasons: 1) most events are *infrequent*; 2) most events are inherently *unscheduled*; and 3) it is often *not known* ahead of time, what kind of events we should seek to find and identify; i.e., we often do not have a prior knowledge about what to look for.

Given the enormous size of measurement data that is generated by micro-PMUs, such as 124,416,000 readings per micro-PMU per day [1], the challenges that we listed above call for developing effective data-driven techniques that are automated and require *minimal prior knowledge*. Addressing this open problem is the focus of this paper.

### B. Summary of Technical Contributions

Given the unknown, infrequent and unscheduled nature of events in micro-PMU measurements, in this paper, we propose an inter-connected unsupervised event detection and unsupervised event clustering method for micro-PMU measurements; followed by a comprehensive analysis of the engineering implications of the events in each of the key clusters that we identify from real-world micro-PMU measurements. The main contributions in this paper are listed as follows:

- A novel unsupervised event detection method is developed based on the concept of Generative Adversarial Networks (GAN) by training deep neural networks. Given the infrequent nature of events in micro-PMU data, the central idea is to train the GAN models to learn the normal behavior and trends in micro-PMU data. Accordingly, any pattern and signatures that deviates from the captured normal characteristics of the micro-PMU data is marked as an event. Real-world results show the effectiveness of the proposed event detection method compared to multiple state-of-the-art methods in the literature.
- A two-step unsupervised clustering method is proposed. In a pre-processing step, events are categorized based on their origin which is obtained from the proposed event detection method. In the second step, in each pre-processed category, a new clustering model is formulated and solved in form of a mixed-integer linear program (MILP). A new rolling based similarity measure, maximum correlation coefficient (MCC), is used to compare any two events. Our method is capable of *active* clustering, i.e., it forms new clusters whenever needed based on new events. Results show the effectiveness of the proposed clustering model compared to the prevalent clustering methods.
- The events in each identified clusters are scrutinized in order to unmask their engineering implications and use

cases. The origin and the cause of the events are identified to determine how they could be of value to the system operator. The proposed unsupervised approach can also identify the frequency of happening and other statistical characteristics of different event types, extract specific events by combining the event clusters' characteristics and time of occurrence; find rare and unusual events, such as faults and incipient failures and new major loads. It can even identify deficiency in micro-PMU data reporting.

### C. Literature Review

The *event detection* component in this paper can be broadly compared with the other data-driven studies such as in [2], [3], [8]–[13]. Some methods are based on principles in statistics. For example, in [2], which we consider as one of the benchmarks for performance comparison in this study, a data-driven statistical event detection method is proposed that is based on absolute deviation around median, combined with dynamic window sizes. There are also methods that are based on principles in machine learning; most of which are either supervised or semi-supervised. That means, they require either full labeling or partial labeling of the events, e.g., in [8], [10]. As for the few event detection methods in the literature that are unsupervised; they are focused on some specific types of events, such as frequency events [12]. In contrast, the event detection method in this paper does *not* require any prior labeling; yet it is broad to cover a wide range of event types.

The *event clustering* component in this paper can be broadly compared with studies such as in [2], [13], [14]. In [14], auto encoder-decoder is used for feature extraction; and the latent space of the auto encoder-decoder is used for supervised event classification. In [2], supervised support vector classification is used to classify the events based on their source location. In [13], different types of voltage sag events are detected based on a threshold, which is defined by voltage magnitude slope per cycle, then k-means and Ward-method clustering are used to identify the characteristics of the voltage sag events. The main limitation in [2], [14] is that they both require prior event labeling. As for the method in [13], it is focused on voltage sag events. In contrast, the event clustering method in this paper does *not* require prior event labeling or any prior knowledge about the events. In fact, it is designed to explore new events even if they do not match any of the existing clusters. Thus, the proposed method is well-suited to unmask meaningful use cases based on the outcome of the proposed unsupervised event detection and unsupervised event clustering methods.

Compared to the conference version of this work in [11], which was *solely about event detection*, this paper has several new contributions. First, the model architecture and the features are different and result in better performance. Second, to identify the type of detected events, an unsupervised two-step clustering model is proposed. Third, together, the proposed unsupervised event detection and clustering methods enable us to expose use cases and applications of the key event clusters.

## II. UNSUPERVISED DETECTION METHOD

The proposed GAN-based event detection method is developed by training two deep neural networks by using real-

world micro-PMU data. In short, the first deep neural network, a.k.a., generator, tries to generate data points that follow the distribution of the real-world data. The second deep neural network, a.k.a., discriminator, tries to distinguish between the generated data points and the real-world data. The architecture and process of the GAN models is as follow:

**A. Features:** Checking the *magnitude* of voltage and current in micro-PMU measurements is a common option to detect and identify events, e.g., see [2], [11], [15]. However, due to the fluctuations in the frequency of the power system, the phase angles of voltage and current are often not used directly. Instead, active power and reactive power are usually used as the two features that involve voltage and current phase angle measurements, besides the magnitude of voltage and current, to detect events in micro-PMU measurements. In this paper, we propose to use power factor as the feature that involves the voltage and current phase angle measurements. Thus, the features across the three phases that we use in this paper are

$$|V_\phi|, |I_\phi|, \cos(\theta_\phi), \quad \phi = A, B, C. \quad (1)$$

which denote the voltage magnitude, current magnitude, and power factor on each phase  $\phi$ , respectively. For notational simplicity, in the rest of paper, we refer to the features in (1) for *all the three phases*, without specifying subscript  $\phi$ .

**B. Generator:** It is a deep neural network that comprises Long Short-Term Memory (LSTM) modules [16] as well as dense layers similar to [11]. Given a noise vector  $z$  from a distribution function  $p_z(z)$ , such as  $z \sim \mathcal{N}(\mu_z, \sigma_z^2)$ , the generator aims to produce samples that follow the distribution of the real-world data. Thus, a neural network  $G(z, \theta_g)$  is trained to minimize the following objective function, where  $\theta_g$  denotes the weights of the generator network [17]:

$$\frac{1}{N} \sum_{i=1}^N [\log(1 - D(G(z_i)))] \quad (2)$$

Here,  $N$  denotes the number of samples in a batch of training data set. Also,  $D$  and  $G$  denote the discriminator function and the generator function, respectively.

**C. Discriminator:** It aims to distinguish between the generated samples by the generator and the actual measurements. It contains LSTM modules and dense layers. Neural network  $D(x, \theta_d)$  is trained to report a single value as output. Here,  $x$  and  $\theta_d$  denote the vector of the measurements and the weights of the discriminator network, respectively. The discriminator maximizes the probability of distinguishing between the measurement and the data generated by the generator, as:

$$\frac{1}{N} \sum_{i=1}^N [\log(D(x_i)) + \log(1 - D(G(z_i)))] \quad (3)$$

where  $x_i$  is the  $i^{th}$  real sample. On one hand, the generator tries to minimize (2). On the other hand, the discriminator tries to maximize (3). Thus, the generator and the discriminator play a *min-max* game over the following function:

$$V(G, D) = \mathbb{E}_{x \sim p_{data}(x)} [\log(D(x))] + \mathbb{E}_{x \sim p_z(z)} [\log(1 - D(G(z)))] \quad (4)$$

**D. Training:** Prior studies have shown that only about 0.04% of micro-PMU measurements contain events [11]. Accordingly, we train all the nine constructed GAN models, one model for each feature, so as to learn characteristics of the normal trends in micro-PMU measurements; and accordingly we detect an event when there is any abnormality. For each GAN model, the optimal value of the min-max game over  $V(G, D)$  in (4) must satisfy the following two conditions:

- **C1:** For any fixed  $G$ , the optimal discriminator  $D^*$  is:

$$D_G^*(x) = \frac{p_{data}(x)}{p_{data}(x) + p_g(x)}. \quad (5)$$

- **C2:** There exists a global solution such that:

$$\min_D (\max(V(G, D))) \iff p_g(x) = p_{data}(x). \quad (6)$$

The training of the GAN model is explained in details in [17].

**E. Event Scoring:** Once all the nine GAN models are trained, they provide us with nine distinct event detectors; one per each feature. Each discriminator gives us a *score* as its output, which indicates how close a given window of measurements is to the global optimum that is obtained from (5) and (6). If, for any GAN model, the score is not close enough to the global optimum, then that means the given window of measurements does *not* match the normal behavior that is learned by the GAN model; thus, it is deemed to contain an event. In this process, a normal probability distribution function (PDF) is fit to the obtained scores for training set, to have  $\zeta \sim \mathcal{N}(\mu, \sigma^2)$ , where  $\mu$  is almost equal to the global optimum and  $\sigma$  is small.

**F. Algorithm:** The proposed event detection method is summarized in Algorithm 1. The algorithm has two phases. First, a learning phase, in which the GAN models are trained for each feature; and their associated normal PDF are constructed. Second, an event detection phase, in which, for each window  $w$  of test data, the scores are calculated by all the nine GAN models and accordingly the *detection vector* is obtained:

$$\mathbf{E}_{9 \times 1}^w = [e_1^w, \dots, e_9^w] \quad (7)$$

The detection vector is a  $9 \times 1$  *binary* vector, where 9 is the number of features as in (1). Entry  $e_f^w$  is 1 if an event is detected in  $w^{th}$  window and  $f^{th}$  feature, otherwise zero. It should be noted that, a common choice for  $z_p$  in the threshold  $\mu \pm z_p \sigma$  is 3, known as the three-sigma rule [18].

The detection vectors not only show us the existence of event; they also provide us with the inputs that we need for our clustering algorithm; which we will explain in Section III.

### III. UNSUPERVISED CLUSTERING METHOD

Given the detection vectors in Section II, in this section, we develop a two-step event clustering method so that we can later study different types of events in details.

#### A. Step I: Pre-Processing

An obvious choice for clustering is to group the events based on their detection vector. For each measurement window  $w$  that contains an event, vector  $\mathbf{E}_{9 \times 1}^w$  has at least one entry that is one. Accordingly, we can put all the events with the

---

#### Algorithm 1 Unsupervised Event Detection

---

**Input:** Training and test data based on the features in (1).  
**Output:** Event Detection vector  $\mathbf{E}_{9 \times 1}^w$  for the  $w^{th}$  test data.

**// Learning Phase**

**ForEach**  $f$  in (1):

- Train the  $GAN_f$  model
- Use discriminator as scoring function  $D_f^*(\cdot)$ .
- Calculate the scores for the training data.
- Fit a Normal PDF  $\mathcal{N}(\mu_f, \sigma_f^2)$  to the obtained scores.

**End**

**// Detection Phase**

**ForEach** new micro-PMU test data ( $w$ ):

**ForEach**  $f$  in (1):

- Calculate score  $s_f^w$  using  $D_f^*(\cdot)$ .
- If**  $s_f^w \notin (\mu_f - z_p \delta_f, \mu_f + z_p \delta_f)$  **Then**  
 $e_f^w = 1$  // Event
- Else**  
 $e_f^w = 0$  // No Event
- End**
- Append  $e_f^w$  to  $\mathbf{E}^w$

**End**

**End**

---

same detection vector in the same category; based on the nine features in (1). For example, we put all the events with  $\mathbf{E}_{9 \times 1}^w = [111\ 000\ 000]$  in the same category because they similarly causes abnormalities only in voltage magnitude on all phases.

In theory the detection vector can result in  $2^9 - 1 = 511$  possible combinations; when an event is detected. However, based on the physics of the power system; only some of these combinations can actually happen in practice. In fact, our analysis of the real-world micro-PMU data resulted in only a handful of such combinations across thousands of detected events; as we will discuss in details in Section IV-B.

Thus, in practice, the above clustering mainly serves as a *pre-processing* in the clustering problem. We often need to further break down a category into several clusters to expose the use case of the events in that category. This is done through a comprehensive clustering optimization in Section III-B.

#### B. Step II: Clustering Optimization

In this section, we explain the similarity measure, the proposed clustering optimization problem formulation, its solution based on exact linearization, the cluster representatives, and the optimum cluster numbers in each category.

**1) Rolling-Based Similarity Measure:** The key to proper clustering is to accurately measure how similar (or dissimilar) different event signatures are within each pre-processed category. However, this is a challenging task because similar events may not have exact same duration. Events need to be aligned with respect to their shape and their corresponding measurement windows for appropriate similarity assessment.

To address the above two challenges, we propose to first expand the measurement window size for each captured event to make sure that the entire event is included in the measurement window. Once this is done, for each event  $i$ , we define:

$$\mathbf{P}_i = \begin{bmatrix} \alpha_i^{1,1} & \dots & \alpha_i^{1,\tau} \\ \vdots & \ddots & \vdots \\ \alpha_i^{9,1} & \dots & \alpha_i^{9,\tau} \end{bmatrix}. \quad (8)$$

There are nine rows in  $\mathbf{P}_i$  corresponding to the nine features in (1). The columns correspond to the measurement time instances, where  $\tau$  is the maximum expanded window size of the two events that are compared with each other.

To determine the similarity between two events  $i$  and  $j$ , we need to align matrices  $\mathbf{P}_i$  and  $\mathbf{P}_j$ , because we do *not* know *where exactly* the event is located within each measurement window. Therefore, we propose to take matrix  $\mathbf{P}_i$  as fixed, and *roll* matrix  $\mathbf{P}_j$  in the time axis, one time slot at a time. In other words, in each rolling step, the last column is removed from  $\mathbf{P}_j$  and appended before the first column in  $\mathbf{P}_j$ ; thus, we have  $\tau$  rolling steps for each two event comparison.

For each rolling step  $k$ , where  $k = 1, \dots, \tau$ , let us define  $c_{i,j}^k$  as the average of the 9 correlation coefficients that can be calculated between each of the 9 rows in  $\mathbf{P}_i$  and its corresponding row in  $\mathbf{P}_j$ ; where  $\mathbf{P}_j$  is rolled for  $k$  steps. We define MCC as the rolling-based measure of similarity as:

$$MCC_{i,j} = \max_{k=1, \dots, \tau} c_{i,j}^k; \quad (9)$$

to be used as the similarity measure between events  $i$  and  $j$ .

2) *Optimization Problem Formulation*: Consider a given category of events based on the pre-processing step in Section III-A. Suppose there are  $I$  detected events in this category and we want to break them down into  $C$  clusters. We propose to solve the following clustering optimization problem:

$$\underset{u}{\text{minimize}} \quad \sum_{i=1}^I \sum_{j=1}^I \sum_{c=1}^C u_{i,c} u_{j,c} (1 - MCC_{i,j}) \quad (10a)$$

$$\text{subject to} \quad u_{i,c} \in \{0, 1\}, \quad (10b)$$

$$\sum_{c=1}^C u_{i,c} = 1 \quad \forall i. \quad (10c)$$

where  $u_{i,c}$  is a binary variable. It is one if event  $i$  is in cluster  $c$ ; otherwise it is zero. Problem (10) minimizes the sum of the distances between the events, measured as  $1 - MCC_{i,j}$ , across different clusters. The constraint in (10c) assures that each event is assigned to only one cluster. Problem (10) is a MINLP.

3) *Exact Linearization*: To enhance computational performance, the MINLP in (10) to an *exact equivalent* Mixed Integer Linear Programming (MILP), as follows:

$$\underset{u, t}{\text{minimize}} \quad \sum_{i=1}^I \sum_{j=1}^I \sum_{c=1}^C t_{i,j,c} (1 - MCC_{i,j}) \quad (11a)$$

$$\text{subject to} \quad u_{i,c}, t_{i,j,c} \in \{0, 1\}, \quad (11b)$$

$$\sum_{c=1}^C u_{i,c} = 1 \quad \forall i, \quad (11c)$$

$$u_{i,c} + u_{j,c} - t_{i,j,c} \leq 1 \quad \forall i, j, c, \quad (11d)$$

$$-u_{i,c} - u_{j,c} + 2t_{i,j,c} \leq 0 \quad \forall i, j, c. \quad (11e)$$

where the nonlinear product of  $u_{i,c}$  and  $u_{j,c}$  in the objective function is replaced with linear term  $t_{i,j,c}$ . The linear constraints

in (11d) and (11e) are used to make sure that  $t_{i,j,c}$  is indeed equal to such product in order to assure an *exact* linearization. Problem (11) can be solved using any MILP solver for a set of detected events in a given time period as training set.

4) *Cluster Representatives*: Once the clusters are obtained by using the training data and solving the MILP problem in (11), we define a representative for each cluster to speed up the process of clustering incoming events. Thus, the new events are compared to a few cluster representatives rather than to all events through (11). To determine the optimum representative for each cluster, we solve the following optimization problem:

$$\underset{v}{\text{minimize}} \quad \sum_{i=1}^I \sum_{j=1}^I \sum_{c=1}^C u_{i,c} v_{j,c} (1 - MCC_{i,j}) \quad (12a)$$

$$\text{subject to} \quad v_{i,c} \in \{0, 1\}, \quad (12b)$$

$$\sum_{i=1}^I v_{i,c} = 1 \quad \forall c \quad (12c)$$

Variable  $v_{j,c}$  is binary. It is one, if event  $j$  is the representative event for cluster  $c$ , and zero otherwise. Constraint (12c) is used to make sure that there is only one representative for each cluster. Notice that  $u_{i,c}$  is parameter, not a variable, in this optimization problem; because the clusters are already formed. Therefore, problem (12) is an MILP by construction.

5) *Number of Clusters*: So far, we have assumed that the number of clusters, i.e., parameter  $c$  is fixed. However, we do obtain the optimal number of clusters in our proposed method. This is done by solving the optimization problem in (11) with respect to different number of clusters. Then, the optimal number of clusters is determined based on the silhouette values of the clusters. Subsequently, cluster representatives are identified for the optimally obtained cluster by using (12).

### C. Active Clustering

Given the large number of events that are detected in micro-PMU measurements, it is computationally prohibitive in practice to re-run the clustering algorithm from scratch every time that a new event is detected. To address this issue, we solved the clustering optimization problem only on the first day in our two weeks test period. On the rest of the days, we actively search for new clusters with respect to the upcoming events if do not appear to belong to the existing clusters.

If MCCs of a new event is less than a threshold for every existing cluster representative, then a new cluster is created. In practice, such new cluster is added only occasionally. Furthermore, the clusters can be updated using the complete optimization-based approach periodically once every few days.

## IV. EXPERIMENTAL RESULTS

The proposed event detection and clustering methods are applied to 1.2 billion measurements over 15 days of real-world micro-PMU data. Fourteen days of data are used for training the event detection method and one day of data is used to test it. One day of data is used for cluster optimization; and active clustering is done for the rest of the data.

TABLE I  
EVENT DETECTION F1-SCORE

Metric	Benchmark [2]	Enhanced Method [11]	Proposed Method
F1-score	0.3614	0.9023	0.9562

TABLE II  
EVENT CLUSTERING F1-SCORE

Distance	KNN	k-medoids	Fuzzy k-medoids	Proposed Method
Euclidean	0.4308	0.5192	0.4967	0.4167
DTW	0.5676	0.8742	0.8753	0.9219
soft-DTW	0.5415	0.8519	0.8724	0.8783
MCC	0.6298	0.8783	0.8724	0.9685

### A. Event Detection Results

The input of every GAN model is a vector of 40 data points and the output is the normality score. Also, in order to assure that events are not overlooked, we consider that each window has 20 data points overlap with the previous window.

Table I shows the F1-score for the proposed event detection method, in comparison with the methods in [2], [11] over 1000 reference events that are visually extracted by expert knowledge to evaluate the performance of event detection. The proposed method outperforms the methods in [2] and [11].

An interesting observation when we compare the proposed event detection model with the model in [11] is that, the choice of the independent features in (1), in particular the use of  $\cos(\theta)$  instead of active power and reactive power, improves the accuracy of event detection. It also improves the independence in the outputs of the trained GAN models. This makes the resulting detection vectors to even enhance the performance of the subsequent clustering method.

### B. Event Clustering Results

The proposed event clustering method is applied to the captured events in Section IV-A; and its performance is compared with the following prevalent clustering methods in the literature: kNN [19], k-Medoids [20], and fuzzy-k-Medoids [21]. Different similarity measures are also considered: euclidean, DTW [22], soft-DTW [23], and MCC. The comparison is conducted over 4000 reference events that are visually clustered with expert knowledge.

Table II shows the F1-score for different clustering methods. Two observations can be made based on the results in this table. First, the clustering methods are almost always more accurate when our MCC is used as the similarity measure. Second, our proposed clustering method outperforms kNN, k-Medoids, and fuzzy-k-Medoids for any similarity measure.

### C. Analysis of Identified Clusters

A total of nine detection vectors were observed among all the events during the test period. They are denoted by  $E_1$  to  $E_9$ , as shown in Table III. As part of the pre-processing step in Section III-A, these detection vectors result in five categories, denoted by Category I to Category V, as shown on the last column in Table III. Categories I, II, and III include *balanced* events; while Categories IV and V include *unbalanced* events.

TABLE III  
CLUSTER CATEGORIES FROM PRE-PROCESSING

Detection Vector	Features	Number of Events	Pre-Processing Category
$E_1$	[111 111 111]	34242	I
$E_2$	[111 000 000]	12270	II
$E_3$	[000 111 111]	809	III
$E_4$	[000 100 100]		
$E_5$	[000 110 110]	13956	IV
$E_6$	[000 011 011]		
$E_7$	[000 000 111]		
$E_8$	[000 000 110]	52	V
$E_9$	[000 000 011]		

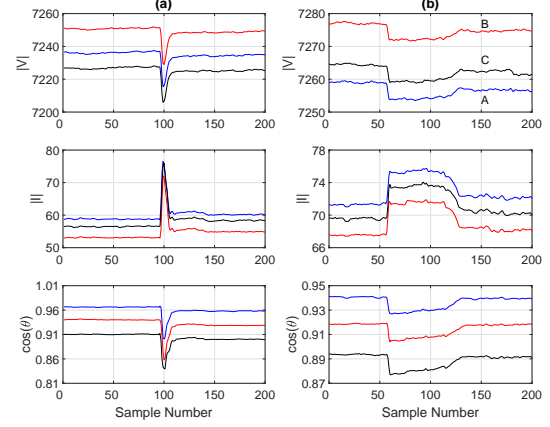


Fig. 1. Examples of load switching events: (a) inrush current in Cluster #1; (b) long transient with a plateau in Cluster #2.

The optimization-based clustering in Section III-B is then applied to the above five categories. It resulted in identifying a total of **16 final clusters**. In this regard, Category I is divided into six clusters; Category II is divided into three clusters; Category III is one cluster by itself; Category IV is divided into three clusters; and Category V is divided into three clusters.

Next, we use the above clustering results to scrutinize and expose the use cases for the events within each cluster.

### D. Use Case Exposition: Six Clusters in Category I

Six clusters are identified in Category I; denoted by Clusters #1 to #6. Clusters #1 and #2 can help identify different load types. Clusters #3 and #4 can reveal malfunctions in the operation of capacitors. Cluster #5 can help identify a specific two-step transient events. Cluster #6 can identify oscillations.

1) *Identifying Different Load Types*: Fig. 1(a) shows an example for Cluster #1, which is the most frequent event in this system. It is the inrush current from load switching. The transient time of these events is less than 10 time slots, i.e., 83.3 msec, and one pinnacle which illustrates the magnitude of inrush current. Fig. 2 shows the scatter plot for the change in the steady-state current, i.e.,  $\Delta(I_{ss})$ , versus the magnitude of inrush current, i.e.,  $|I_{inr}|$  during 6 different days. As it can be seen, Cluster #1 can it self be divided into two main sub-clusters which show two major types of loads in this cluster.

Fig. 1(b) shows an example for Cluster #2. It is for the load types that create much longer transient period to switch and creates a *plateau*; which is very different from the inrush current in Cluster #1 with a *pinnacle*. Fig. 3 shows a scatter plot for the events in Cluster #2. On the y-axis it shows the change in steady-state current, before and after the event, which is

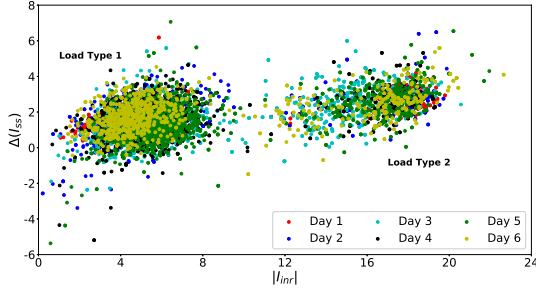


Fig. 2. Identifying two major load types based on Cluster #1.

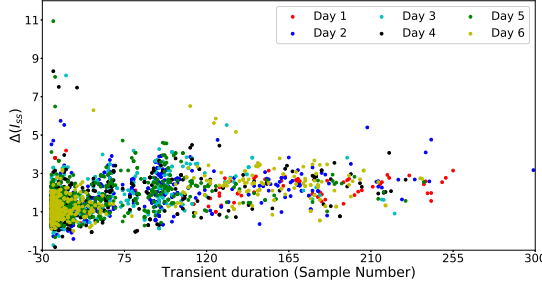


Fig. 3. Scatter plot for the events in Cluster #2 over 6 days.

denoted by  $\Delta(I_{ss})$ . The x-axis is the length of the transient period of the event. There is a dense concentration area, where  $\Delta(I_{ss})$  fluctuates at around 1.5 A. This observation empowers the system operator to more readily detect any abnormalities in this cluster, with regard to  $\Delta(I_{ss})$  and transient duration, such as multiple simultaneous load switching.

2) *Capacitor Bank State of Health Monitoring*: Figs. 4(a) and (b) show examples of clusters #3 and #4, which are related to capacitor bank switching ‘on’ and switching ‘off’ events, respectively. Capacitor bank switching occurs on a daily basis.

Monitoring the switching actions of capacitors can not only keep the utility operator informed of switching status of the capacitor banks; it can also help to evaluate their state of health. For example, consider the capacitor bank switching off event in Fig. 4(b). We can see that there is a relatively long *overshoot* on Phase A current and a relatively long *undershoot* on Phase B current before the capacitor is de-energized. This is likely due to a *malfunction* in the switching control mechanism at the capacitor bank, c.f. [4]. By clustering all the capacitor switching events, we can conduct statistical analysis on the characteristics of such transient switching responses and dispatch the field crew to examine the capacitor bank switching controller and perform repairs.

3) *Two-step Events*: Fig. 5 shows an example of the special load in Cluster #5. This special type of load has two separate but subsequent steps. By using the proposed unsupervised event detection and unsupervised event clustering method we were able to capture it and identify its unique switching pattern that is repeated every time this event occurs.

4) *Oscillations in Current Induced by Step Changes*: Fig. 6 shows an example of an oscillation event in Cluster #6. These events always occur immediately after a particular pattern of a step up change event in the current magnitude (as we can see at the beginning of the Fig. 6(a)) that also is followed by an

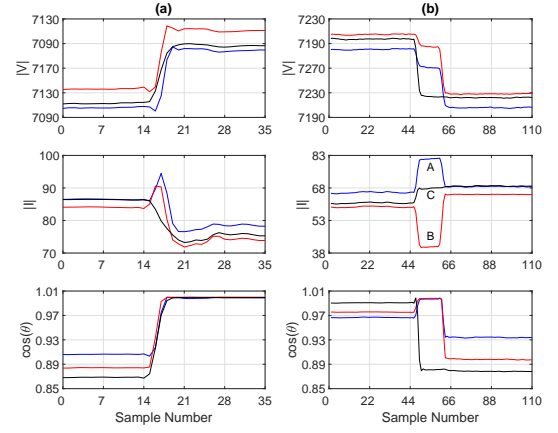


Fig. 4. Monitoring the operation and health of a capacitor bank based on Clusters #3 and #4: (a) switch on; (b) switch off.

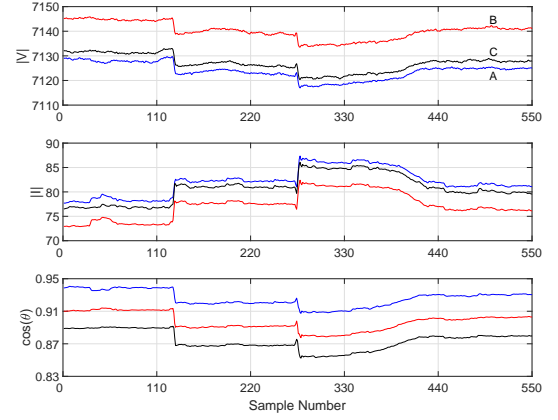


Fig. 5. An example for the two-step event in Cluster #5.

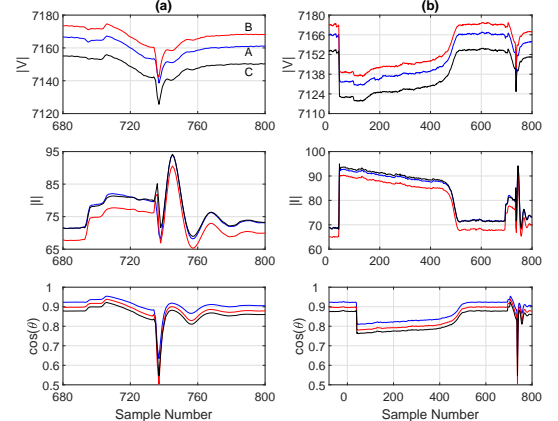


Fig. 6. An example for the oscillation event in Cluster #6: (a) oscillation in current; (b) the step change prior the oscillations.

oscillation event which is magnified in Fig. 6(b). The average oscillation frequency is 5.2 Hz and with 2.97% damping ratio. This type of event causes the *highest transient power factor* change at this distribution feeder, when compared with all kinds of events that we have captured in this study. The amount of the transient change in power factor is 0.4.

#### E. Use Case Exposition: Three Clusters in Category II

Three clusters are identified in Category II; denoted by Cluster #7 to Cluster #9. Clusters #7 and #8 can help identify

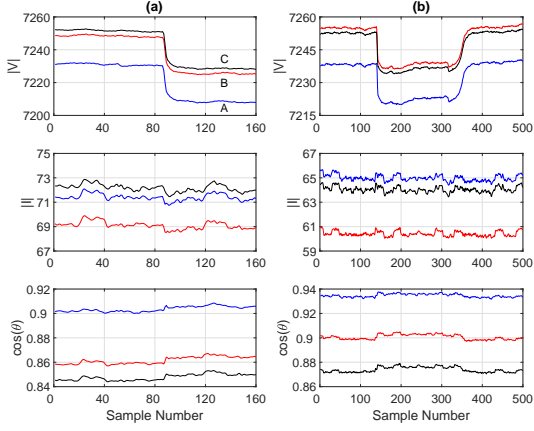


Fig. 7. Examples of voltage events: (a) transformer tap-changer in Cluster #7; (b)

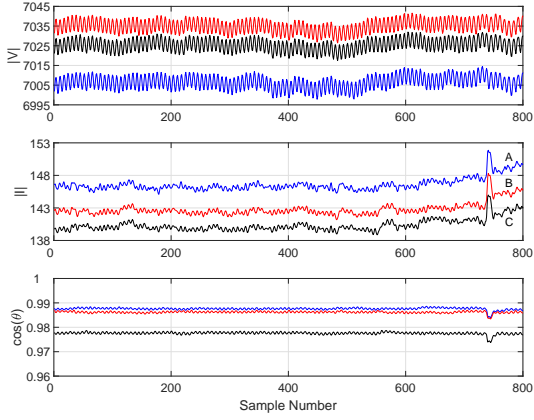


Fig. 8. An example for voltage oscillation event in Cluster #9.

voltage events. Cluster #9 can identify voltage oscillations.

1) *Voltage Events*: Fig. 7(a) shows an example of Cluster #7, which is a transformer tap changing event. The events in this cluster inform the utility about voltage regulation status and the operation of tap-changers. Fig. 7(b) shows an example event in Cluster #8, which is a voltage event with a *plateau*. The transient shape of the voltage in Cluster #8 is similar to voltage changes in Cluster #2, see Fig. 1(b); however, these two events are different because there is no change in current phasors ( $|I|$  and  $\cos(\theta)$ ) in the events in Cluster#8. The events in Clusters #7 and #8 are often initiated at transmission level.

2) *Voltage Oscillation Events*: Fig. 8 shows an example for an event in Cluster #9, which is a high frequency low magnitude event in  $|V|$ . Since there is no major change in current, this event can be due to two possible phenomena: 1) voltage oscillation from the upstream system; 2) temporary malfunction in micro-PMU data reporting. The later can be considered as a possibility if it persists and if other micro-PMUs do not report a similar behavior. In that case, this can be used as an indicator to request micro-PMU diagnostics.

#### F. Use Case Exposition: One Cluster in Category III

One cluster is identified in Category III; denoted by Cluster #10. Fig. 9 shows an example for this cluster. The events in this cluster affect only the current magnitude and power factor, rather than the voltage magnitude. It should be noted that, the pre-processing step in the proposed two-step clustering method

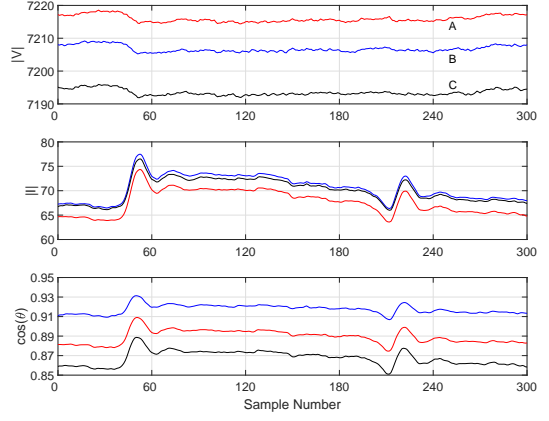


Fig. 9. An example for current oscillation event in Cluster #10.

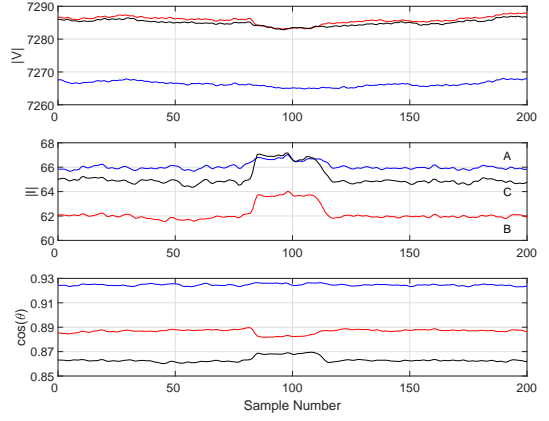


Fig. 10. An example for the unbalanced events in Cluster #11. The event affects the current magnitude of phases B and C.

helps to distinguish the events in Cluster #10 from the events in Clusters #2 and #5, despite their relatively high MMC.

#### G. Use Case Exposition: Three Clusters in Category IV

Three clusters are identified in Category IV; denoted by Clusters #11 to #13. The events in these clusters are *unbalanced*. Fig. 10 shows an example of the event in Cluster #11. This event is *not* detected by the event detection method in [11]; because that method fails to notice small changes in just one feature, i.e. in  $|I_B|$ . However, in our method, by using one GAN model for each feature, even small events are detected.

#### H. Use Case Exposition: Three Clusters in Category V

Three clusters are identified in Category V; denoted by Clusters #14 to #16. They are all related to power factor events. An example for an event in Cluster #14 is shown in Fig. 11. It shows oscillations in power factor. There are also some minor oscillations, in the magnitudes of current and voltage during the same period. Other types of power factor events are also captured by the clusters in this category; not shown here.

#### I. Special Sequence of Events

One of the applications of the proposed unsupervised methods is to analyze the shape, occurrence time and sequence of the detected and clustered events. Our analysis shows that certain events come in sequence. This is an important observation to enhance the predictability of the system, its

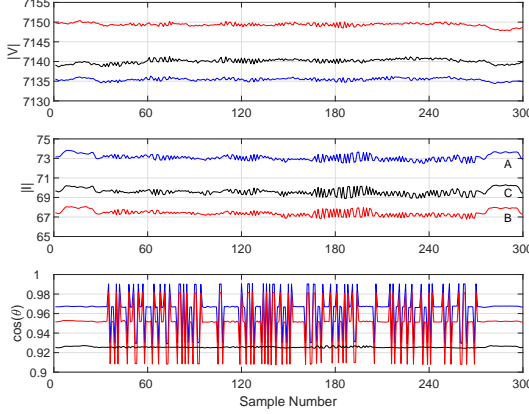


Fig. 11. An example for power factor event in Cluster #14.

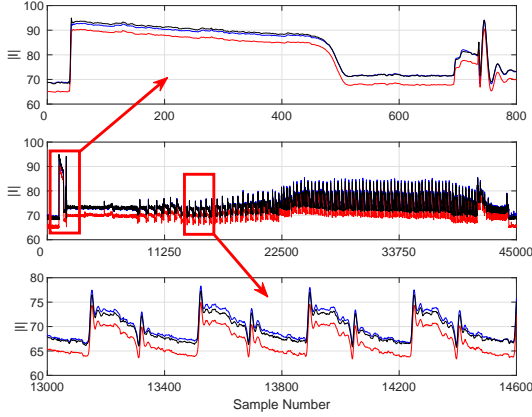


Fig. 12. An example for the special sequence of the events in the current magnitude that are repeated occasionally. It was captured based on the collaboration of Clusters #6 and #10.

dynamics, and its events. An example is shown in Fig. 12. It is a *super event* which consists of a sequence of several smaller events that belong to Clusters #6 and #10. This super event is first triggered by an event that belongs to Cluster #6, which we previously saw in Fig. 6. Then, after about 60 seconds, a series of over 100 events occur that all belong to Cluster #10. This sequence continues with a growing amplitude until it goes away. The exact same sequence of events occurred on the same day and around the same time each week.

## V. CONCLUSIONS

A set of new unsupervised methods are proposed to detect and cluster different types of events in micro-PMU measurements. The proposed methods need *minimal prior human knowledge* of events. The test results based on real-world micro-PMU data confirm that the proposed event detection method, which works based on training a novel GAN model, outperforms the existing, in particular when it comes to detecting the events that may impact only a subset of the features or only a subset of the phases. Test results also show the effectiveness of the proposed two-step clustering method, compared to the other prevalent methods, due to the proposed choice of the similarity measure and also the proposed architecture that improves clustering accuracy. Moreover, the active nature of the proposed clustering method makes it capable of identifying new clusters of events on *an ongoing basis*. Variety

of event clusters are scrutinized in details in order to unmask different use cases for the utility operator.

## REFERENCES

- [1] H. Mohsenian-Rad, E. Stewart, and E. Cortez, "Distribution synchrophasors: Pairing big data with analytics to create actionable information," *IEEE Power and Energy Magazine*, vol. 16, no. 3, pp. 26–34, May 2018.
- [2] A. Shahsavari, M. Farajollahi, E. Stewart, E. Cortez, and H. Mohsenian-Rad, "Situational awareness in distribution grid using micro-pmu data: A machine learning approach," *IEEE Trans. on Smart Grid*, vol. 10, pp. 6167–6177, Nov. 2019.
- [3] Y. Seyed, H. Karimi, and S. Grijalva, "Irregularity detection in output power of distributed energy resources using pmu data analytics in smart grids," *IEEE Trans. on Industrial Informatics*, vol. 15, no. 4, pp. 2222–2232, 2018.
- [4] A. Shahsavari, M. Farajollahi, E. Stewart, A. von Meier, L. Alvarez, E. Cortez, and H. Mohsenian-Rad, "A data-driven analysis of capacitor bank operation at a distribution feeder using micro-pmu data," in *Proc. of the IEEE PES ISGT*, Washington, DC, Feb. 2017.
- [5] E. M. Stewart, V. Hendrix, M. Chertkov, and D. Deka, "Integrated multi-scale data analytics and machine learning for the distribution grid and building-to-grid interface," Lawrence Livermore Lab, Tech. Rep., 2017.
- [6] A. Shahsavari, M. Farajollahi, E. Stewart, E. Cortez, and H. Mohsenian-Rad, "A machine learning approach to event analysis in distribution feeders using distribution synchrophasors," in *IEEE PES SGSMA*, 2019.
- [7] M. Farajollahi, A. Shahsavari, E. M. Stewart, and H. Mohsenian-Rad, "Locating the source of events in power distribution systems using micro-pmu data," *IEEE Trans. on Power Systems*, vol. 33, no. 6, pp. 6343–6354, 2018.
- [8] Q. Cui and Y. Weng, "Enhance high impedance fault detection and location accuracy via  $\mu$ -pmus," *IEEE Trans. on Smart Grid*, vol. 11, no. 1, pp. 797–809, 2019.
- [9] S. Liu, Y. Zhao, Z. Lin, Y. Liu, Y. Ding, L. Yang, and S. Yi, "Data-driven event detection of power systems based on unequal-interval reduction of pmu data and local outlier factor," *IEEE Trans. on Smart Grid*, vol. 11, no. 2, pp. 1630–1643, 2020.
- [10] Y. Zhou, R. Arghandeh, and C. J. Spanos, "Partial knowledge data-driven event detection for power distribution networks," *IEEE Trans. on Smart Grid*, vol. 9, no. 5, pp. 5152–5162, Sep. 2018.
- [11] A. Aligholian, A. Shahsavari, E. Cortez, E. Stewart, and H. Mohsenian-Rad, "Event detection in micro-pmu data: A generative adversarial network scoring method," in *IEEE PES General Meeting*, August 2020.
- [12] N. Duan and E. M. Stewart, "Frequency event categorization in power distribution systems using micro pmu measurements," *IEEE Transactions on Smart Grid*, vol. 11, no. 4, pp. 3043–3053, 2020.
- [13] T. J. Swenson, E. Vrettos, J. Müller, and C. Gehbauer, "Open  $\mu$ pmu event dataset: Detection and characterization at lbnl campus," in *IEEE PES General Meeting (PESGM)*, 2019.
- [14] Y. Tang and J. Yang, "Dynamic event monitoring using unsupervised feature learning towards smart grid big data," in *IJCNN*, May 2017.
- [15] M. Jamei, A. Scaglione, C. Roberts, E. Stewart, S. Peisert, C. McParland, and A. McEachern, "Anomaly detection using optimally placed  $\mu$ PMUsensors in distribution grids," *IEEE Trans. on Power Systems*, vol. 33, no. 4, pp. 3611–3623, July 2018.
- [16] S. Hochreiter and J. Schmidhuber, "Long short-term memory," *Neural Comput.*, vol. 9, no. 8, p. 17351780, Nov. 1997.
- [17] I. Goodfellow, J. Pouget-Abadie, M. Mirza, B. Xu, D. Warde-Farley, S. Ozair, A. Courville, and Y. Bengio, "Generative adversarial nets," in *Proc. of NIPS*, Montreal, Canada, Dec. 2014.
- [18] F. Pukelsheim, "The three sigma rule," *The American Statistician*, vol. 48, no. 2, pp. 88–91, 1994.
- [19] J. MacQueen, "Some methods for classification and analysis of multivariate observations," in *proc. of the Berkeley Symposium on Mathematical Statistics and Probability*, Berkeley, CA, 1967.
- [20] L. Kaufman and P. Rousseeuw, *Clustering by Means of Medoids*, ser. Delft University of Technology : reports of the Faculty of Technical Mathematics and Informatics, 1987.
- [21] R. Krishnapuram, A. Joshi, O. Nasraoui, and L. Yi, "Low-complexity fuzzy relational clustering algorithms for web mining," *IEEE Trans. on Fuzzy Systems*, vol. 9, no. 4, pp. 595–607, Aug 2001.
- [22] D. J. Berndt and J. Clifford, "Using dynamic time warping to find patterns in time series," in *KDD Workshop*, 1994.
- [23] M. Cuturi and M. Blondel, "Soft-DTW: a differentiable loss function for time-series," in *Proc. of International Conference on Machine Learning*, Sydney, Australia, Aug 2017.